The Effects of Damköhler Number in a Turbulent Shear Layer

by

J. E. Broadwell and M. G. Mungal*

Graduate Aeronautical Laboratories
California Institute of Technology
Pasadena, CA 91125

4 June 1986

GALCIT Report FM86-01

*Present Affiliation:
Department of Mechanical Engineering
Stanford University
Stanford, CA 94305

Abstract

A simple model describing chemical reaction in a turbulent shear layer is put in quantitative form and the model predictions compared with experiment. The reactants are not pre-mixed and the flow is two-dimensional. The dependence of the amount of product in the layer on the Schmidt, Reynolds, and Damköhler numbers and on the stoichiometric ratio is exhibited explicitly in the model. The first two parameters appear as the product (Sc Re) and influence that part of the reaction taking place in strained laminar flames. In the limit $Sc\,Re \to \infty$ (for $Sc > 1$ and $Re \gg 1$) the molecular mixing becomes independent of these parameters as it is in classical turbulence theory but the composition and spatial distribution of the molecularly mixed fluid does not resemble those given by such theories. The model predictions are in reasonable agreement with the experimental results for a Damköhler number range from zero to a mixing limited value. The comparison with a set of data for gases in which Re was varied is somewhat less satisfactory.

I. Introduction

This paper presents the results of an analytical study of chemical reactions in a two-dimensional turbulent shear layer. In particular, the experimental results for the variable rate hydrogen-fluorine reaction reported by Mungal and Frieler in Ref. 1 are interpreted in terms of the model proposed in Ref. 2. The reaction takes place between H_2 and nitric oxide, NO, carried in a high speed nitrogen stream and F_2 in a low speed nitrogen stream. In most of the experiments the high and low speed velocities were 22 m/sec and 8.8 m/sec but several runs were made at 44 m/sec and 17.6 m/sec. The H_2 concentration is eight percent molar, the F_2 concentration is one percent molar, and that of the NO (needed to initiate the reaction) varies between 0 and 0.03 percent molar. A description of the apparatus and of the experiment is given in Ref. 1.

The important reactions are:

$$F + H_2 \xrightarrow{k_1} HF + H \tag{1}$$

$$F_2 + H \xrightarrow{k_2} HF + F \tag{2}$$

$$F_2 + NO \xrightarrow{k_3} NOF + F \tag{3}$$

described by the equations:

$$\frac{d[H_2]}{dt} = -k_1 [F] [H_2]$$

$$\frac{d[F_2]}{dt} = -k_2 [F_2] [H] - k_3 [NO] [F_2]$$

$$\frac{d[NO]}{dt} = -k_3 [F_2] [NO]$$

It was shown in Ref. 1 that this kinetic system behaved as if it were a single reaction

$$H_2 + F_2 \xrightarrow{k} 2\ HF \tag{4}$$

governed by the rate equation

$$\frac{d[HF]}{dt} = k [H_2][F_2] \tag{5}$$

where k is a function of the initial nitric oxide concentration, $[NO_i]$. In the following we make use of this approximation, i.e., we assume a single reaction governed by a rate constant k.

Because the reactant concentrations are low, the density changes are neglected and the fluid motion is assumed to be unaffected by the chemical reaction.

II. Physical Ideas

The ideas on which the model is based come from a series of experiments beginning with those of Brown & Roshko[3]. Most, in fact, derive from this now widely known seminal study. The subsequent work of Konrad[4], Breidenthal[5] and Brown & Dimotakis[6] and the analyses of Corcos and Sherman[7] provided further evidence for the basic concepts. This evidence is discussed in detail in Ref. 2 and a model suggested by the observations is proposed in qualitative terms. Here the physical ideas will be reviewed briefly, the model will be put in quantitative form, and results from it compared with the experimental findings. Finally, shortcomings of the model are discussed and possible improvements suggested.

The experiments cited above show that the sequence of events by which parcels of fluid from the two streams reach the molecularly mixed state begin when the fluid elements are entrained into the shear layer by large scale coherent motions. The parcels are distributed across the layer and are entangled (using Roshko's term) by vortical motions in large scale structures. This motion, molecular mixing, and chemical reaction are governed by the equations, in non-dimensional form:

$$\nabla \cdot V^* = 0 \tag{6}$$

$$\frac{\partial V^*}{\partial t^*} + V^* \cdot \nabla V^* = \frac{1}{Re} \nabla^2 V^* - \nabla p^* \tag{7}$$

$$\frac{\partial \alpha_i}{\partial t^*} + V^* \cdot \nabla \alpha_i = \frac{1}{ReSc} \nabla^2 \alpha_i - \omega^*_i \qquad (8)$$

in which $V^* = V/\Delta u$, $p^* = p/\rho_\infty(\Delta u)^2$, $x_i^* = x_i/\delta$, $t^* = t(\Delta)/\delta)$, $Sc = \nu/D$, $Re = \Delta u\, \delta/\nu$, α_i is the mole fraction and ω_i^* the dimensionless chemical reaction term. Here Δu is the velocity difference $(u_1 - u_2)$ and δ the local layer thickness. We take the Schmidt number, Sc, to be of order unity or larger and the Reynolds number, Re, to be large. It is conventional, and presumably justifiable, at large Re to ignore the effects of the viscous terms in Eq. (7) on the motion. For the molecular mixing, however, the diffusion term is essential. In view of the nature of Eq. (8), especially in the limit $Re \to \infty$, it seems plausible that thin diffusive layers, boundary layers in the mathematical sense, would form between fluid from the two streams and that their thickness, ℓ, would be of the order $\delta/(Sc\,Re)^{1/2}$. In the model, these layers are represented by the solutions for the laminar diffusion zones formed in stagnation point flows, conventionally called strained flames.

It is argued next that as a structure moves downstream, the laminar mixing layers are lengthened and further intertwined as ever smaller scales are generated. This (Lagrangian) motion is taken to be a Kolmogorov-like cascade to λ_0, the Kolmogorov scale. When the fluctuations reach this scale, the layers merge. (During this motion, the structures are distorted and may intermingle, so that when the layers merge they do not necessarily form large, distinguishable regions in the cores as Fig. 5 in Ref. 2 may unfortunately suggest.) Since the

time to diffuse across the scale $\lambda_0 \sim \delta/Re^{3/4}$, is of the order $(\delta/\Delta u) \cdot Sc/Re^{1/2}$, at high Re the molecules in the layers interdiffuse in a time that is short compared to the cascade time, $\delta/\Delta u$, to form what is called in the model, the homogeneous mixture. Because the layers in a given structure have been distributed throughout the mixing layer by the large scale motion before they merge, we assume that the homogeneous mixture has a composition that is nearly independent of the lateral coordinate, y. Additional experimental evidence supporting this approximation is contained in the results of Mungal & Dimotakis[8], and especially, Koochesfahani[9] and Koochesfahani & Dimotakis[10]. In the model, as a further idealization, the homogeneous mixture composition is taken to be a single value: it is assumed to be composed of fluid from the two streams in the ratio, E, the ratio of high speed to low speed fluid entrained into the mixing layer.

The flame sheet area per unit volume, S, computed in the cascade by taking $S \sim 1/\lambda$, where λ in the fluctuation scale, for $\delta > \lambda > \lambda_0$, behaves as intuition suggests, i.e., S increases slowly at first and then extremely rapidly as $\lambda \to \lambda_0$. This behavior is the motivation for dividing the molecularly mixed fluid into two distinct states, flame sheets and the homogeneous mixture. In the model, then, S is the flame sheet area per unit volume at the large scale and is taken, consequently, to scale with $1/\delta$ and to be independent of Re. (The thickness, however, as already noted, depends on Re as well as Sc.)

This description of the flow, involving as it does the motion of large scale fluid elements, pictures the flow to be unsteady at spatial and temporal scales δ and $\delta/\Delta u$. Evidence for such unsteadiness is clear in the temperature-time traces in Ref. 1. In the further development of the model, however, we will be concerned only with mean values and will put the ideas, which were most naturally described in Lagrangian terms, into Eulerian form.

The ideas presented above can be summarized and clarified with the help of the diagram in Fig. 1 which is intended to represent the three fluid states in the shear layer and to show the sequence by which fluid elements pass from one to the other. Also indicated explicitly is the presence of unmixed fluid within the layer. The v's are volume fluxes per unit length into the various states, with v_1 and v_2 the fluxes from the high and low speed streams into the layer. (The entrainment ratio, E (> 1), is v_1/v_2.)

When the molecular diffusion coefficients of the contituents are equal, the flame sheets consist of equal volumes from the two streams. The excess high speed fluid, therefore, becomes part of the homogeneous mixture, directly, at the end of the cascade.

The homogeneous mixture volume flux increases with axial distance x by the addition of a volume flux per unit length, v_h, the sum of the flame sheet flux, v_f and of high speed fluid, v_d. It is easy to show that v_h is made up of v_d and v_f in the proportions

$$v_d = \frac{E-1}{E+1} v_h \quad ; \quad v_f = \frac{2}{E+1} v_h \, .$$

The justifications for the assumption that v_h is a constant independent of Re (to be determined, implicitly, by experiment as shown later) are discussed in Ref. 2; these are, essentially, the same as those given above for dividing the mixed fluid into the two states. The result is that the amount of homogeneously mixed fluid rises linearly with x as does the entrained fluid.

This description of the flow is shown schematically in Fig. 2 in which the cross-hatched regions represent the homogeneous mixture and the thin lines the flame sheets. In the present formulation it is assumed that the flame sheets are formed only between pure fluid from the two streams and, in addition, that their structure and composition is in quasi-equilibrium with the local large scale strain. (In Ref. 2 it is wrongly stated that these properties are in equilibrium with the strain at the small scales.)

III. Model Formulation

In the experiments to be discussed, the amount of product in the shear layer is characterized by the "product thickness", δ_p, defined at a particular axial measuring station by

$$\delta_p = \int_{-\infty}^{\infty} \frac{C_p(y)}{C_\infty} \, dy$$

where C_p is the molar product concentration and C_∞ is the reactant concentration in one of the streams, here taken to be the low speed fluorine bearing stream. Following the discussion above, the contributions of the flame sheets and the homogeneous mixture are considered separately as follows:

$$\delta_p = \int_{-\infty}^{\infty} \frac{C_p}{C_\infty} \, dy = \int_{-\infty}^{\infty} \frac{(C_p)_h}{C_\infty} \alpha(x,y) \, dy + \int_{-\infty}^{\infty} \frac{(C_p)_f}{C_\infty} \ell \cdot S \, dy \quad (9)$$

where $(C_p)_h$ and $(C_p)_f$ denote the homogeneous mixture and average flame sheet product concentrations, in moles per unit volume of homogeneously mixed fluid and of flame sheet fluid, respectively. The fractional volume of homogeneously mixed fluid is denoted by $\alpha(x,y)$ and that of the flame sheet by $\ell \cdot S$ where ℓ is the sheet thickness.

As already noted, $(C_p)_h$ is independent of y at fixed x and $\alpha(x,y) = \alpha(\eta)$, where $\eta = y/\delta$ and δ is the shear layer thickness, here taken to be distance between the one percent of maximum of the product profiles. The homogeneous mixture term can, consequently, be written

$$\frac{(C_p)_h}{C_\infty}\,\delta \int_{-\infty}^{\infty} \alpha(\eta)\, d\eta \ .$$

Carrier, Fendell, and Marble[11] show that $\ell = a(D/\varepsilon)^{1/2}$ where a is a constant of order one, D is the molecular diffusion coefficient, and ε the strain rate. As stated above, we take ε to be the large scale strain, $\Delta u/\delta$ and assume that ℓ and $(C_p)_f$ are also independent of y at fixed x. Since S scales with $1/\delta$, we put $S = \beta(\eta)/\delta$ and write for the flame sheet term

$$\frac{(C_p)_f}{C_\infty}\,\ell \int_{-\infty}^{\infty} \beta(\eta)\, d\eta = a\,\frac{(C_p)_f}{C_\infty}\left(\frac{D\delta}{\Delta u}\right)^{1/2} \int_{-\infty}^{\infty} \beta(\eta)\, d\eta$$

$$= \frac{a\cdot(C_p)_f}{C_\infty}\,\delta(ScRe)^{-1/2} \int_{-\infty}^{\infty} \beta(\eta)\, d\eta$$

With these expressions, Eq. (9) becomes

$$\frac{\delta_p}{\delta} = A\,(C_p)_h/C_\infty + B\,(Sc\ Re)^{-1/2}\,(C_p)_f/C_\infty \qquad (10)$$

where $A = \int_{-\infty}^{\infty} \alpha(\eta)\, d\eta$ and $B = a \int_{-\infty}^{\infty} \beta(\eta)\, d\eta$ are constants to be determined as described later.

Observe that A and B have to do only with the molecular mixing; all the chemical kinetic effects appear in $(C_p)_h$ and $(C_p)_f$. Strictly, A and B must be determined for each free stream velocity and density ratio. It is likely, however, from the arguments leading to the model, that they are weak functions of these variables.

In the next two sections, methods for determining $(C_p)_h$ and $(C_p)_f$ are derived, with the flame sheets considered first.

IV. Strained Flames

A two-dimensional strained flame is formed when two streams carrying reactants meet at a stagnation point as sketched in Fig. 3. Under our conditions, the overall conservation equation is

$$\frac{\partial u}{\partial x} + \frac{\partial v}{\partial y} = 0$$

If v is a linear function of y,

$$v = -\varepsilon y \quad , \quad \frac{\partial u}{\partial x} = -\varepsilon \tag{11}$$

When ε is constant and the reaction is fast relative to diffusion, the reaction takes place on a plane parallel to x and the exact solution of Ref. 11 is available. For finite reaction rates numerical computation is required[12]. While such computations could be used here, it is instructive, instead, to use the approximate solution developed next.

A boundary layer integral approach applied to the control volume indicated by dashed lines in Fig. 3 yields the desired results. To obtain a simple approximate solution, we specialize from the beginning to large values of the ratio $(C_H)_\infty/(C_F)_\infty = 1/\phi$, where ϕ is the stoichiometric ratio (following the conventions of Ref. 8) and where the subscripts H and F denote hydrogen and fluorine. Further, consider only average values for the concentrations in the control volume. Note first that from Eqs. (11) $v(-\ell/2) = \varepsilon\, \ell/2$ and $u = \varepsilon\, \Delta x$.

The conservation equations for H_2 and F_2 in the control volume are

$$-v(+\ell/2)\ (C_H)_\infty\ \Delta x - k(C_F)_f\ (C_H)_f \cdot \ell \cdot \Delta x = (C_H)_f\ \varepsilon\ \ell \cdot \Delta x \quad (12)$$

$$v(-\ell/2)\ (C_F)_\infty\ \Delta x - k(C_F)_f\ (C_H)_f\ \ell \cdot \Delta x = (C_F)_f\ \varepsilon\ \ell \cdot \Delta x \quad (13)$$

From Eq. (12),

$$(C_H)_f = \frac{1}{2}\ \frac{(C_H)_\infty}{\left[1 + \frac{k}{\varepsilon}\ (C_F)_f\right]}$$

Putting this expression into Eq. (13), and solving for $(C_F)_f$ in the limit $(C_F)_\infty \to 0$ (to approximate $(C_H)_\infty/(C_F)_\infty \gg 1$) we get

$$(C_F)_f = \frac{1}{2}\frac{(C_F)_\infty}{\left[1 + \frac{k(C_H)_\infty}{2\,\varepsilon}\right]} \quad (14)$$

In the same limit,

$$(C_H)_f = \frac{(C_H)_\infty}{2}\ . \quad (15)$$

The product concentration, $(C_P)_f$, is obtained from the control volume concentration equation

$$k(C_F)_f\ (C_H)_f\ \Delta x \cdot \ell = u(C_P)_f\ \ell = \varepsilon\ \Delta x (C_P)_f\ \ell$$

which becomes, using Eq. (14) and (15),

$$(C_P)_f = \frac{k(C_H)_\infty}{4\varepsilon} \frac{(C_F)_\infty}{\left[1 + \frac{k(C_H)_\infty}{2\varepsilon}\right]} \tag{16}$$

a result consistent with the requirement that

$$(C_P)_f + (C_F)_f = (C_F)_\infty/2 \ .$$

To compare these results with the exact solution of Ref. 11, note first that since $\ell = a(D/\varepsilon)^{1/2}$, the amount of product per unit flame sheet area, $\kappa_P = (C_P)_f \cdot \ell$ is, from Eq. (16) with $k \to \infty$, given by

$$\kappa_P = (a/2)\ (C_F)_\infty\ (D/\varepsilon)^{1/2} \tag{17}$$

The exact solution is

$$\kappa_P = (2/\pi)^{1/2}\ (\phi+1)\ e^{-\Lambda^2}\ (C_F)_\infty\ (D/\varepsilon)^{1/2} \tag{18}$$

where $\Lambda = \mathrm{erf}^{-1}\ \frac{(\phi+1)}{(\phi-1)}$. Thus the dependence on the parameter (D/ε) is the same in the two expressions.

For small k, Eq. (16) reduces to

$$(C_P)_f = \frac{(C_H)_\infty\ (C_F)_\infty}{4}\ (k/\varepsilon)$$

a result in agreement with the analysis of Norton[13].

In summary, Eqs. (15) and (16) are approximations for all k for $(C_H)_\infty/(C_F)_\infty = 1/\phi \gg 1$, while Eq. (18) is the exact solution for $\frac{k(C_H)_\infty}{\varepsilon} \gg 1$ for all ϕ.

Arguments were given above for taking ε proportional to $\Delta u/\delta$. Variation of the proportionality constant around unity had so little effect on the overall results that unity was chosen for convenience in the following work.

V. The Homogeneous Mixture

In this section expressions for the reactant and product concentrations in the homogeneous mixture are developed. First, an expression for the flux of the homogeneously mixed fluid is written and then the fluorine conservation equation is derived.

The homogeneous mixture flux, V_h, can be written

$$V_h = \int_{-\infty}^{\infty} \alpha(y)\, u(y)\, dy = \delta \int_{-\infty}^{\infty} \alpha(\eta)\, u(\eta)\, d\eta$$

where α has the same meaning as before. To avoid introducing an additional unimportant constant, we approximate the above integral by writing

$$V_h = \delta\, \bar{u} \int_{-\infty}^{\infty} \alpha(\eta)\, d\eta = \delta\, \bar{u}\, A \tag{19}$$

where $\bar{u} = (u_1 + u_2)/2$. Therefore, this flux increases linearly with x and is equal to $v_h x$ as indicated in Fig. 1, i.e.,

$$\delta\, \bar{u}\, A = v_h\, x \tag{20}$$

When fluorine is carried in the low speed stream, no fluorine "enters" the V_H flux directly, it is homogenized only after becoming part of a flame sheet. The fluorine and hydrogen conservation equations for the homogeneous mixture are, under these conditions,

$$\frac{d}{dx}\int_{-\infty}^{\infty}(C_F)_h\,\alpha(y)\,u(y)\,dy = -\int_{-\infty}^{\infty}k(C_H)_h\,(C_F)_h\,\alpha(y)\,dy + \frac{2(C_F)_f}{E+1}\,v_h \tag{21}$$

$$\frac{d}{dx}\int_{-\infty}^{\infty}(C_H)_h\,\alpha(y)\,u(y)\,dy = -\int_{-\infty}^{\infty}k(C_H)_h\,(C_F)_h\,\alpha(y)\,dy + \left[\frac{2}{E+1}\,(C_H)_f + \frac{(E-1)}{(E+1)}\,(C_H)_\infty\right] v_h \tag{22}$$

Equation (21) describes the change in the fluorine flux in the mixture caused by the consumption of F_2 in the chemical reaction and the addition from the flame sheets. Using Eq. (19) and (20), we find,

$$\frac{d}{dx}\left[x(C_F)_h\right] = \frac{-k(C_H)_h\,(C_F)_h\,x}{\bar{u}} + \frac{2(C_F)_f}{E+1} \tag{23}$$

$$\frac{d}{dx}\left[x(C_H)_h\right] = \frac{-k(C_H)_h\,(C_F)_h\,x}{\bar{u}} + \left[\frac{2}{(E+1)}\,(C_H)_f + \frac{(E-1)}{(E+1)}\,(C_H)_\infty\right] \tag{24}$$

The approximation used in the flame sheet analysis, i.e., that the hydrogen depletion by chemical reaction can be neglected is introducted next. With $(C_H)_f = (C_H)_\infty/2$, Eq. (24) yields

$$(C_H)_h = \frac{E}{(E+1)}\,(C_H)_\infty\,, \tag{25}$$

The hydrogen from the free stream is again simply diluted in the

homogeneous mixture by the low speed free stream fluid.

With this result Eq. (23) becomes

$$\frac{d}{dx^*}\left[(x^*(C_F)_h\right] = -\frac{E}{(E+1)}\, x^*(C_F)_h + \frac{2(C_F)_f}{(E+1)} \qquad (26)$$

where $x^* = k\,(C_H)_\infty\, x/\bar{u}$.

Since $\epsilon = \Delta u/\delta$, in which Δu is simply related to $\bar{u}$ and $\delta = 0.16x$, Eq. (14) shows that $(C_F)_f$, also, is a function of x^* only. Equation (26) can, therefore, be solved by standard methods to yield $(C_F)_h$ as a function of x^* and, since

$$(C_P)_h/C_\infty + (C_F)_\infty/C_\infty = 1/(E+1)\ , \qquad (27)$$

the variation of the product concentration at the (fixed x) measuring station with the reaction rate. Interestingly, the over-all solution is dependent only upon the Damköhler-like variable, x^*, which arises naturally in the analysis.

It is helpful to note that when $x/\bar{u}$ is replaced by t in Eqs. (23) and (24), they become equations describing exactly the fluorine and hydrogen concentrations in a homogeneous (ie., well-stirred) reactor to which streams of flame sheet and free stream fluid are being steadily added.

VI. Comparison of Theory & Experiment

To compare the theoretical predictions with the experimental results of Ref. 1, values for the constants A and B are required. They have already been determined by Mungal & Dimotakis[8] from their data for fast chemical reactions. For completeness, the constants will be rederived here, in a slightly different way, with essentially the same results. In any event, no re-adjustments are made (nor are possible) to fit the variable chemical rate data of Ref. 1.

The most straight-forward and accurate procedure makes use of two sets of results: (1) the first from a run for a nominal NO concentration in Ref. 1 and (2) from the study of Koochesfahani & Dimotakis[10] of a fast chemical reaction in water. We need not be concerned here with the details of the later experiment, needing only to note that it was for $Re = 2.2 \cdot 10^4$, $\phi = 1/10$, and $Sc = 600$.

The HF experiment, for $Re = 6.6 \cdot 10^4$ and $\phi = 1/8$ yielded $\delta_p/\delta = 0.24$ and the water experiment gave $\delta_p/\delta = 0.13$.

Eq. (10) repeated from Section III, i.e.,

$$\frac{\delta_p}{\delta} = A\,(C_p)_h/C_\infty + B(ScRe)^{-1/2}\,(C_p)_f/C_\infty \qquad (10)$$

is applicable to both experiments.

For the liquid reaction $k \gg 1$ and Eqs. (26) and (16) can be used to find that $(C_P)_h/C_\infty = 1/(E + 1)$ and $(C_P)_f/C_\infty = 0.5$. For the F_2/H_2 fast reaction experiment, $k(C_H)_\infty = (0.53 \cdot 10^{-3}\ \text{sec})^{-1}$ and $\varepsilon = 176\ \text{sec}^{-1}$. We have, again using Eqs. (26), (27) and (16), $(C_P)_h/C_\infty = .997/(E + 1)$ and $(C_P)_f/C_\infty = 0.42$. With these values and $E = 1.3$, Eq. (10) applied to the two experiments yields $A = 0.28$ and $B = 64.5$.

Substitution of these values into Eq. (10) shows that the product in the gas at this Reynolds number is almost equally divided between the homogeneous mixture and the flame sheets.

The expression for finite chemical reaction rate is, therefore,

$$\frac{\delta_P}{\delta} = 0.28\ (C_P)_h/C_\infty + 64.5(\mathrm{Re})^{-1/2}\ (C_P)_f/C_\infty$$

where Sc has been put equal to unity and the quantities $(C_P)_h/C_\infty$ and $(C_P)_f/C_\infty$ are to be found from Eqs. (26), (27) and (16). Figure 4 compares the analytical and experimental results. It shows the normalized product thickness at the measuring station in terms of the Damköhler number Da, where $Da = k\ C_{H_\infty}\ s/\bar{u}$ and s is the distance between the measuring station, x = 47.7 cm, and the location of the shear layer transition to fully developed turbulence, x = 15 cm. The contributions of the homogeneous zones and the flame sheets indicated separately, show that in contrast to the homogeneous mixture, the product concentration in the flame sheet approaches its asymptotic value slowly: even at Da - 60, the reaction is not quite mixing-limited. While, as can be

seen, the agreement between the experiment and the predictions of the model is satisfactory, experiments over a wider range of conditions are needed to test the model more stringently.

It is useful next to discuss effects of the Reynolds number on this reaction because when Re is increased by increasing the velocities, there is an accompanying change in the Damköhler number. Fig. 5 shows the theoretical results for several values of the reaction rate together with the recent measurements of Mungal et al.[14] The curve marked $k/k^* = 1$ is to be compared with the experimental values. That for infinite reaction rate, $k/k^* = \infty$, illustrates the effect of Reynolds number alone. The Reynolds number range in the experiments is too limited to permit definite conclusions from the comparison at this time.

The analysis in this paper has been concerned primarily with the effects of Damköhler and Reynolds number on chemical reactions in turbulent shear layers. The application of the model to reactions in which the equivalence ratio was varied is discussed by Mungal and Dimotakis.[8]

VII. *Concluding Remarks*

We conclude with a tentative explanation of the data in Fig. 7 of Ref. 1 showing that the slope of the ramps in the temperature-time traces within the structures at high chemical reaction rate decreases as the rate is lowered becoming nearly zero at the lowest rate. Simultaneously, the asymmetry in the time-mean temperature profile disappears: Fig. 3a, Ref. 1. Observe first from Fig. 4 that the relative contribution of the flame sheets to the product declines as the reaction rate is reduced. Next Koochesfahani[12] found that in liquids, where (in the present view) the flame sheet contribution is negligible, the time-mean profiles of the product concentration are symmetric and ramps are not present in the concentration-time traces. These observations are consistent with the idea that the ramps and asymmetries are associated with flame sheets.

In the model, the sheets are formed between pure fluids from the two streams, consequently their composition is the same everywhere. This over-simplification must, therefore, be dropped if the observations described above are to be explained by reference to the flame sheet composition. The required generalization is that the newly entrained fluids form mixing layers not only between themselves but with the homogeneous fluid. Mungal and Dimotakis[9] suggest such a generalization. After reviewing the evidence that high speed fluid enters the structures along their high speed and downstream boundaries and the low speed fluid along the low speed and upstream edges, they propose that the two

streams mix, to some degree, with the homogeneous fluid as they enter. The resulting flame sheet compositions are such as to explain the observed ramp and mean profile characteristics.

These ideas may be stated another way: at finite Reynolds number, mean product profiles are symmetric and there are no ramps when the molecular mixing is delayed, i.e., does not occur in the flame sheets. In gases, this can be the consequence of a low reaction rate; in liquids, slow molecular diffusion is the cause. In the limit $(Sc\,Re) \to \infty$ (with $Sc > 1$ and $Re \gg 1$) the flame sheet thickness goes to zero; consequently liquids and gases behave similarly. That the model approaches a limit in which the mixing is independent of Re and Sc is in accord with classical turbulence theory but the distribution and composition of the mixed fluid are qualitatively different.

Ramp-like features have been observed in scalar time traces in a wide variety of experiments in the laboratory[15,16] and in the atmosphere[17]. A more extensive review of these earlier studies and a comparison with the present work is in preparation.

Acknowledgement

The authors wish to acknowledge many helpful discussions with their GALCIT colleagues and especially to thank Richard Miake-Lye for his specific valuable comments on the manuscript. This work was sponsored jointly by the Air Force Office of Scientific Research under Grant No. 83-0213 and the Office of Naval Research under Contract No. N00014-76-C-0260.

REFERENCES

1. Mungal, M. G. and Frieler, C. E.: "The Effects of Damköhler Number on a Turbulent Shear Layer - Experimental Results", GALCIT Report No. FM85-01, California Institute of Technology, Pasadena, CA, 31 December 1985.

2. Broadwell, J. E. and Breidenthal, R. E.: J. Fluid Mech. 125, 397 (1982)

3. Brown, G. L. and Roshko, A.: J. Fluid Mech. 64, 775. (1974).

4. Konrad, J. H.: An Experimental Investigation of Mixing in Two-Dimensional Turbulent Shear Flows with Application to Diffusion-Limited Chemical Reactions, Ph.D. thesis, California Institute of Technology, 1976; also available as Project SQUID Tech. Rep. CIT-8-PU, 1976.

5. Breidenthal, R. E.: J. Fluid Mech. 109, 1 (1982).

6. Dimotakis, P. E. and Brown, G. L.: J. Fluid Mech. 78, 535 (1976).

7. Corcos, G. M. and Sherman, F. S.: J. Fluid Mech. 73, 241 (1976).

8. Mungal, M. G. and Dimotakis, P. E.: J. Fluid Mech. 148, 349 (1984).

9. Koochesfahani, M. M.: Experiments on Turbulent Mixing and Chemical Reactions in a Liquid Mixing Layer, Ph.D. thesis, California Institute of Technology, 1984.

10. Koochesfahani, M. M. and Dimotakis, P. E.: AIAA J. 23(11), 1700 (1985).

11. Carrier, G. F., Fendell, F. E. and Marble, F. E.: SIAM J. Appl. Math. 28(2), 463 (1975)

12. Dixon-Lewis, G., et al.: Twentieth Symposium (International) on Combustion, p. 1893, The Combustion Institute, 1984.

13. Norton, O. P.: The Effects of a Vortex Field on Flames with Finite Reaction Rates, Ph.D. thesis, California Institute of Technology, 1983.

14. Mungal, M. G., Hermanson, J. C. and Dimotakis, P. E.: AIAA J. 23(9), 1418 (1985).

15. Fiedler, H. F.: Adv. Geophy. 18A, 93, (1974).

16. Fiedler, H. F.: Turbulent Mixing in Nonreactive and Reactive Flows, A Project SQUID Workshop, p. 381, Plenum, 1975.

17. Gibson, C. H., Friehe, C. A. and McConnell, S. O.: Phys. Fluids 20(10), Part II, S156 (1977).

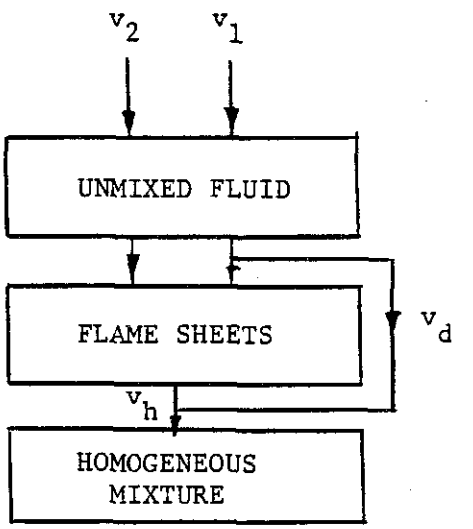

Figure 1. Fluid states in shear layer.

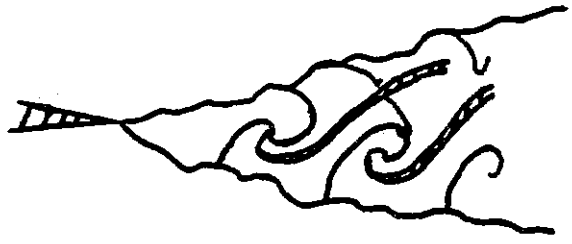

Figure 2. Strained flame sheets (solid lines) and homogeneously mixed zones (cross-hatched) in shear layer.

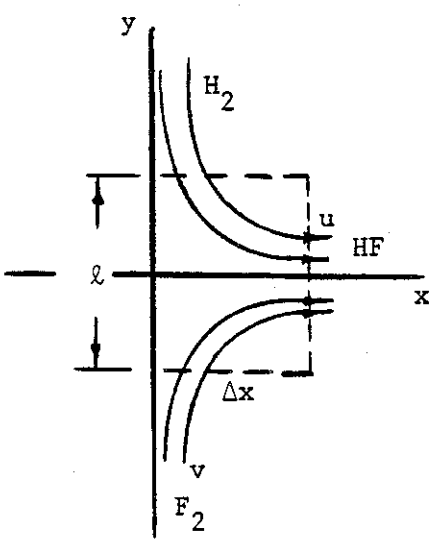

Figure 3. Strained flame control volume.

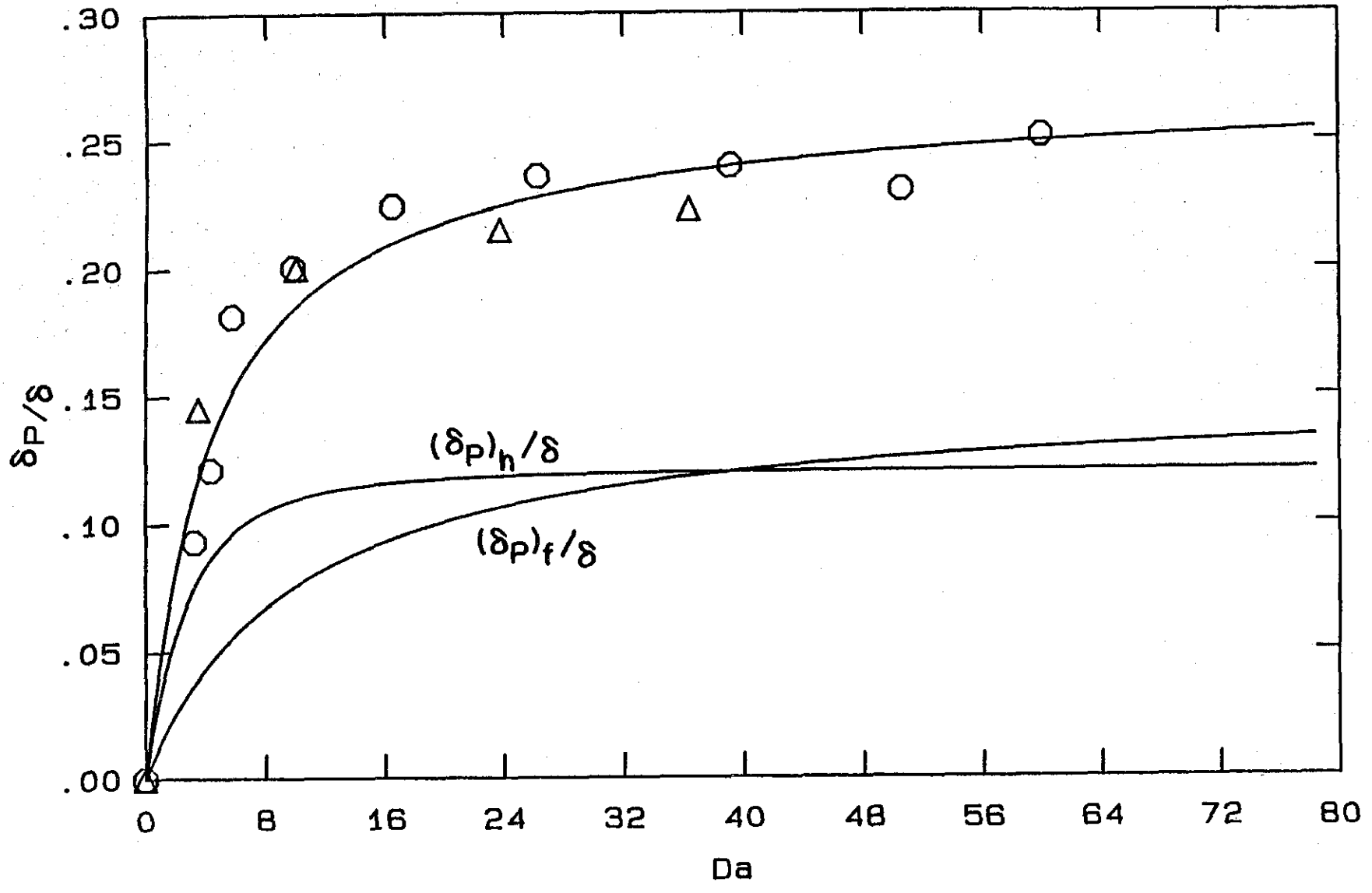

Figure 4. Dependence of product thickness on Damköhler number, Da = k C_{H_∞} s/$\bar{u}$. δ_P, total product; $(\delta_P)_f$, flame sheet product; $(\delta_P)_h$, homogeneous mixture product; δ, shear layer thickness; O , experiment[1], u_1 = 22 m/sec, u_2 = 8.8 m/sec; Δ u_1 = 44 m/sec, u_2 = 17.6 m/sec.

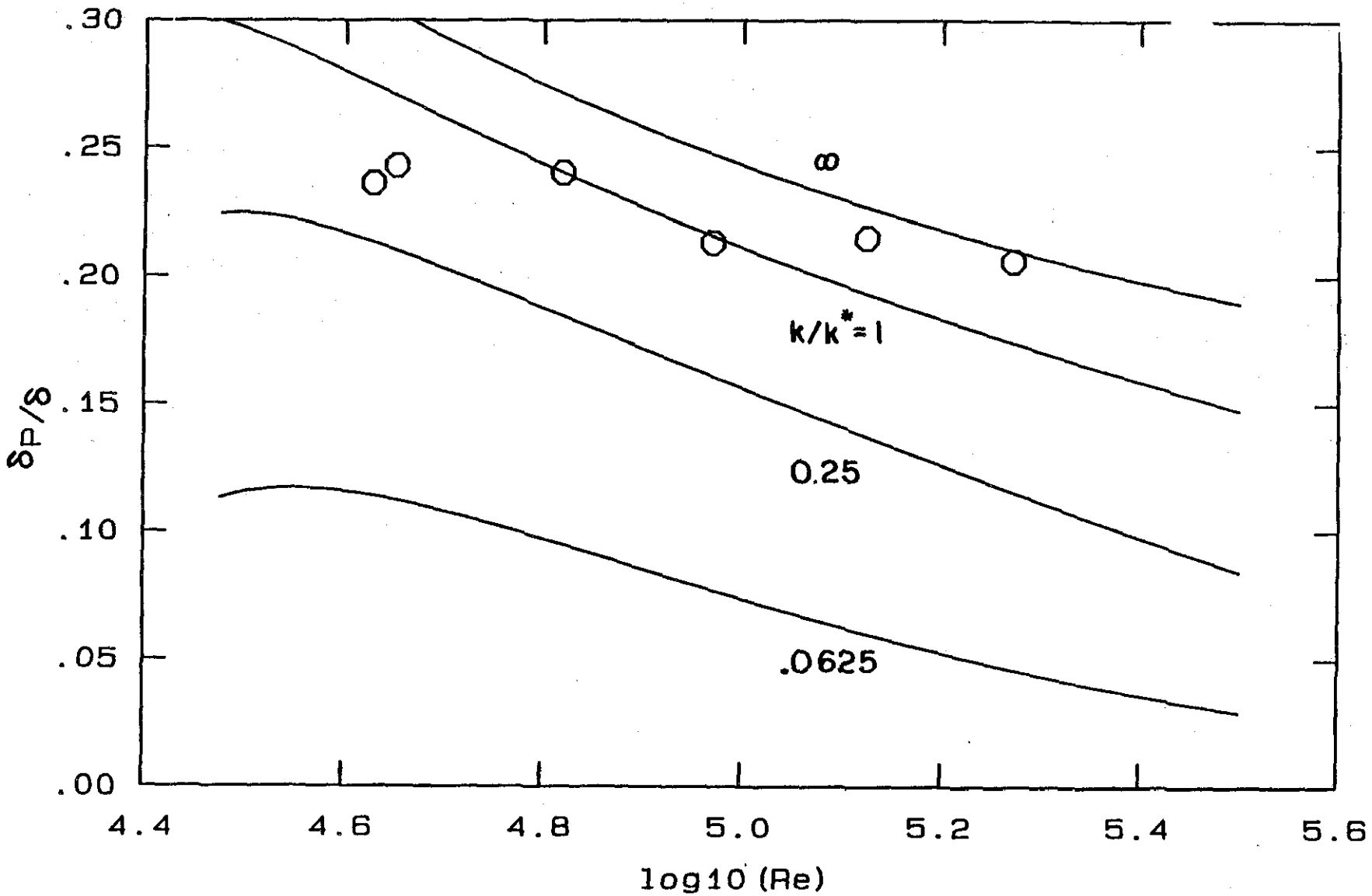

Figure 5. Dependence of product thickness on Reynolds number for various reaction rates. $(C_H)_\infty k^* = (0.53 \cdot 10^{-3}\ \text{sec})^{-1}$. O experimental results from Mungal, Hermanson and Dimotakis[14].